Available online at www.sciencedirect.com

ScienceDirect

Advances in Space Research 67 (2021) 921–929

ADVANCES IN SPACE RESEARCH (a COSPAR publication)

www.elsevier.com/locate/asr

# On how atmospheric temperature affects the intensity of oxygen emissions in the framework of the Barth's mechanism

Valentine Yankovsky

*Atmospheric Physics Department, Saint Petersburg State University, 7/9 Universitetskaya nab, Saint Petersburg 199034, Russia*

Received 13 July 2020; received in revised form 16 November 2020; accepted 19 November 2020
Available online 7 December 2020

**Abstract**

The three-body recombination of oxygen atoms $O + O + M \rightarrow O_2(el) + M$ is the dominant process of oxygen excitation in the Earth's nightglow at altitudes of 85–110 km. The rate coefficient of this reaction, as well as the quantum yields of electronically excited products ($O_2$(el) in the electronic states: $^5\pi_g$, $A^3\Sigma_u^+$, $A'^3\Delta_u$, $c^1\Sigma_u^+$, $b^1\Sigma_g^+$, $a^1\Delta_g$, $X^3\Sigma_g^-$) depend on the gas kinetic temperature. In addition to the direct one-stage excitation channel of these levels of the $O_2$ molecule, the Barth's mechanism considers the two-stage energy transfer channel. In this channel, higher excited levels of the $O_2$ act as precursors for the excitation of the O($^1$S) atom and the underlying electronic levels of the $O_2$. In this study, we use sensitivity analysis to consider the temperature dependence of the processes of excitation and quenching for each of the excited components. The analytical expressions are obtained for the sensitivity coefficients of the Volume Emission Rates depending on temperature for the green line of atomic oxygen O($^1$S → $^1$D), the Herzberg I band $O_2(A^3\Sigma_u^+ \rightarrow X^3\Sigma_g^-)$ and $O_2$ Atmospheric band $O_2(b^1\Sigma_g^+, v' = 0 \rightarrow X^3\Sigma_g^-, v'' = 0)$. With the help of the sensitivity analysis performed in this work, we (a) confirm that the state $O_2(^5\pi_g)$, produced by the three-body recombination of atomic oxygen, is a precursor for the formation of $O_2(b^1\Sigma_g^+)$, (b) estimate the quantum yield of the $O_2(b^1\Sigma_g^+)$ state formed as a result of collisional reaction $O_2(^5\pi_g)$ with $O_2$, and (c) propose a method for determining a type of precursor for production of O($^1$S) in the Barth's mechanism.
© 2020 COSPAR. Published by Elsevier Ltd. This is an open access article under the CC BY-NC-ND license (http://creativecommons.org/licenses/by-nc-nd/4.0/).

*Keywords:* Nightglow; Barth's mechanism; Sensitivity analysis; Herzberg I band; Green line; $O_2$ Atmospheric band

## 1. Introduction

The Barth's mechanism is the dominant source of oxygen nightglow emissions in the upper mesosphere and lower thermosphere (Krasnopolsky, 1987, 2011). The source of the oxygen excitation in this altitude range is the exothermic three-body reaction of the recombination of oxygen atoms

$$O + O + M \rightarrow O_2(el) + M + 5.12 \text{ eV} \quad (1)$$

The rate coefficient of this reaction depends on temperature (Campbell and Gray, 1973)

$$k(O;O;M) = (4.7 \pm 0.4) \cdot 10^{-33} \cdot (T/300)^{-2} \text{ cm}^6 \text{ s}^{-1} \quad (2)$$

In general case, any of following $O_2$ electronic states, $O_2(el)$, can form as a result of the reaction (1): $^5\pi_g$, $A^3\Sigma_u^+$, $A'^3\Delta_u$, $c^1\Sigma_u^+$, $b^1\Sigma_g^+$, $a^1\Delta_g$, $X^3\Sigma_g^-$. Next, we will also use the simplified notation for excited levels: $^5\pi$, $A^3\Sigma$, $A'^3\Delta$, $c^1\Sigma$, $b^1\Sigma$, $a^1\Delta$, $X^3\Sigma$, respectively. All of them are below the dissociation threshold of the oxygen molecule. The rate coefficients of these states production, $k(O;O;M \rightarrow el)$, as a function of kinetic temperature were calculated by Wraight in 1982 and moreover, the calculated total rate of the reaction (1), $k(O;O;M \rightarrow Total)$, was scaled by author to fit the experimental measured value of $k(O;O;M) = 1.12 \cdot 10^{-32}$ cm$^6$ s$^{-1}$ at T = 196 K (Campbell and Gray, 1973). We show the digitized data from (Wraight, 1982) in

*E-mail addresses:* vyankovsky@gmail.com, valentine.yankovsky@spbu.ru

https://doi.org/10.1016/j.asr.2020.11.019
0273-1177/© 2020 COSPAR. Published by Elsevier Ltd.
This is an open access article under the CC BY-NC-ND license (http://creativecommons.org/licenses/by-nc-nd/4.0/).

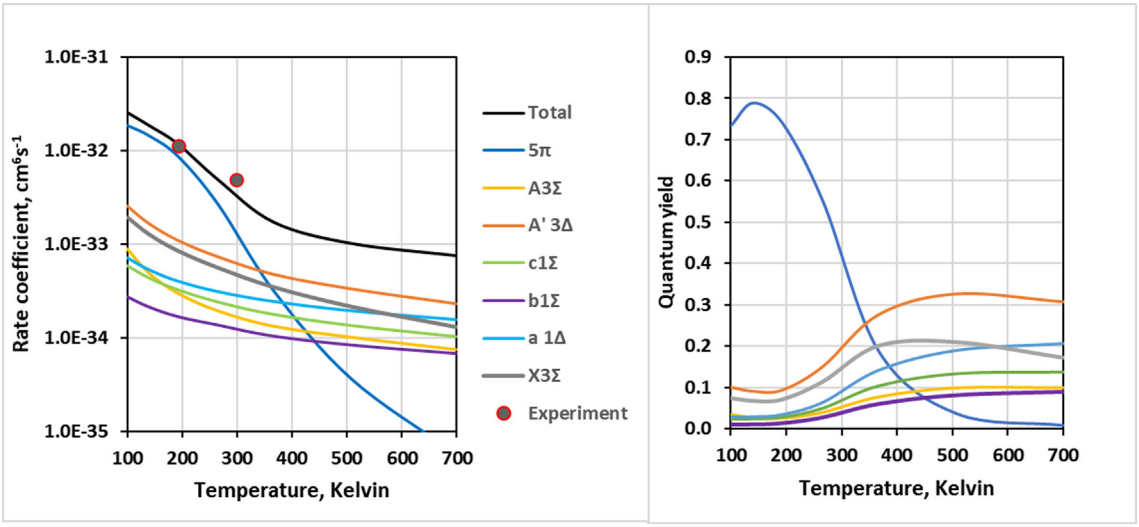


Fig. 1. Left panel - rate coefficients of $O_2$ electronic states production, $k(O;O;M \rightarrow el)$, in the three-body recombination of oxygen atoms (1) depending on temperature (from Wraight, 1982). Right panel - quantum yields of these electronic states based on data from the left panel according (3).

Fig. 1 (the left panel). In practice, most of authors use the total rate coefficient (2) and the quantum yields of the products of the reaction (1). The fixed values of the quantum yields are estimated based on work (Wraight, 1982) for a temperature of about 200 K. However, following this work, the quantum yields have a significant temperature dependence (see Fig. 1). In the right panel of Fig. 1, we present the quantum yields of the $O_2(el)$ calculated based on Wraight's data as follows

$$F(O_2(el)) = \frac{k(O;O;M \rightarrow el)}{k(O;O;M \rightarrow Total)} \tag{3}$$

As known, the Barth's mechanism is usually considered for the nightglow in the altitude range of 85–110 km. In this region, the kinetic gas temperature typically extends in the 140–370 K range (see Fig. 1A in Appendix). Therefore, precisely this temperature range is chosen for studying the dependence of quantum yields of the reaction (1) products on temperature. For an analytical description of the temperature dependence of these quantum yields in the range of T = 140–370 K, we use the exponential fitting function of the form (see Fig. 2).

$$F(O_2(el)) = \omega_{el} \cdot exp\left(\frac{T}{\theta_{el}}\right) \tag{4}$$

where $\omega_{el}$ and $\theta_{el}$ are the fitting constants.

The obtained fitting parameters with coefficients of determination are given in Table 1. Fig. 2 presents the result of calculations by (4) for seven $O_2$ electronic states (dotted lines) versus quantum yields calculated by (3) (solid lines).

The structure of the paper is as follows. Section 2 describes a procedure of excited oxygen components formation in the framework of Barth's mechanism. In Section 3 we construct the sensitivity coefficient for the two-channel Barth's mechanism depending on the gas temperature. In Section 4 we discuss the temperature dependence of the processes of excitation and quenching

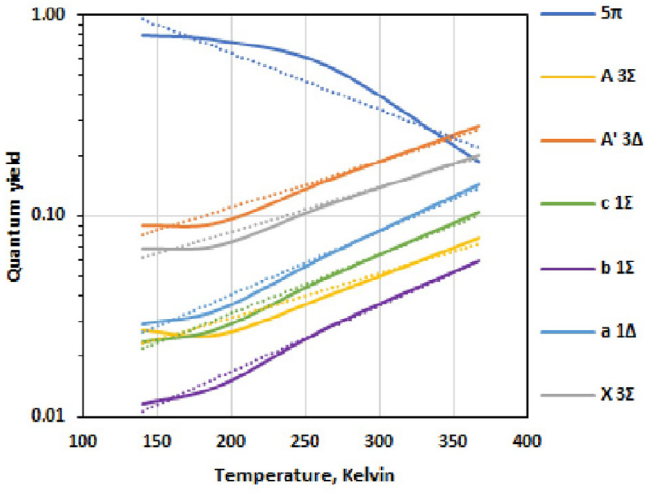


Fig. 2. The quantum yields of $O_2$ electronic states in the reaction (1) calculated according to (3) (solid lines) and their trends calculated using an exponential fitting function (4) (dotted lines) in the temperature range of 140–370 K.

Table 1
Parameters of the fitting function (4) for the quantum yield of $O_2(el)$ electronic states in reaction (1) calculated in this work. The temperature range is 140 – 370 K. $R^2$ is the coefficient of determination.

| Product of the reaction (1) | Designation, el | $\omega_{el}$ | $\theta_{el}$, K | $R^2$ |
|---|---|---|---|---|
| $O_2(5\pi_g)$ | 5π | 2.3419 | −155 | 0.896 |
| $O_2(A^3\Sigma_u^+)$ | A3Σ | 0.0114 | 199 | 0.924 |
| $O_2(A'^3\Delta_u)$ | A′3Δ | 0.0386 | 190 | 0.961 |
| $O_2(c^1\Sigma_u^+)$ | c1Σ | 0.0085 | 148 | 0.984 |
| $O_2(b^1\Sigma_g^+)$ | b1Σ | 0.0037 | 133 | 0.989 |
| $O_2(a^1\Delta_g)$ | a1Δ | 0.0095 | 138 | 0.984 |
| $O_2(X^3\Sigma_g^-)$ | X3Σ | 0.0304 | 198 | 0.966 |

for excited components such as $O(^1S)$, $O_2(b^1\Sigma)$, $O_2(A^3\Sigma)$ at night conditions as a function of altitude. The Summary is presented in Section 5. In Appendix, we discuss altitude profiles of the gas temperature in the upper mesosphere and lower thermosphere and present a database of photochemical processes used in the work.

## 2. Barth's mechanism fundamentals

In this section, when describing the details of modeling the Barth's mechanism, we use the results of analytical studies from McDade et al., Bates, later works by Murtagh up to the recent publications of Grygalashvyly et al. etc. (McDade et al., 1986; Bates, 1988, 1992; Murtagh et al., 1990; Grygalashvyly et al., 2019; Lednyts'kyy and von Savigny, 2020).

Note that all subsequent balance equations and expressions derived from them are obtained for local conditions (in $cm^{-3}$). Therefore, we will not further focus on the relationship between the concentration of excited components and the Volume Emission Rate (VER) originating from them, since relevant databases on Einstein's coefficients are in the public domain (Krupenie, 1972; Bates, 1989; Yankovsky et al., 2019).

The two-channel Barth's mechanism includes both direct excitation of an arbitrary electronic level of an oxygen molecule in reaction (1) and a two-stage formation process of electronic states $O_2$(el): $A^3\Sigma_u^+$, $A'^3\Delta_u$, $c^1\Sigma_u^+$, $b^1\Sigma_g^+$, $a^1\Delta_g$, $X^3\Sigma_g^-$. The efficiency of a direct one-stage process in the three-body recombination of oxygen atoms is described by the quantum yield $F(O_2(el))$ (see Fig. 2, as well as Table 1). The second channel of Barth's mechanism is implemented in two stages. At the first stage, the excited state of the oxygen molecule is formed in the reaction (1). In this case, this excited state is called the precursor. As follows from a large number of works since 1977 (Saxon & Liu, 1977; Wraight, 1982; Klotz and Peyerimhoff, 1986; Partridge et al., 1991, series of Bates' papers in ending of 80; Krasnopolsky, 2011 etc.), the precursor is the oxygen molecule $O_2(\,^5\pi_g)$ which has an excitation threshold just a few hundredths of the electron-volt below the $O_2$ dissociation threshold of 5.12 eV.

Since the $O_2(^5\pi_g)$ quintet state has no radiative transitions to the lower singlet and triplet states, energy from this level is believed to be quenched in collisions with $O_2$ and $O$ ($^3$P). Rate coefficients of these reactions are denoted as $k$ ($O_2(^5\pi_g)$; $O_2$) and $k(O_2(^5\pi_g); O(^3P))$, respectively. The balance equation for $O_2(\,^5\pi_g)$ is

$$\left[O_2(\,^5\pi_g)\right] = \frac{[O]^2[M]\cdot k(O;O;M)\cdot F\left(O_2(\,^5\pi_g)\right)}{[O_2]\cdot k\left(O_2(\,^5\pi_g);O_2\right)+[O]\cdot k\left(O_2(\,^5\pi_g);O\right)} \tag{5}$$

At the second stage, energy from $O_2(^5\pi_g)$ precursor is spent on the excitation of lower energy states of molecular oxygen as a result of collisions with oxygen molecules

$$O_2(\,^5\pi_g)+O_2 \rightarrow O_2(el)+O_2 \tag{6}$$

The quantum yield of the $O_2(el)$ production in reaction (6) is denoted as $\varphi\,(^5\pi_g \rightarrow el)$. Considering both aforementioned channels of the Barth's mechanism, we get the balance equation for the $O_2(el)$formation as follows

$$[O_2(el)] = \frac{[O]^2[M]\cdot k(O;O;M)}{Q(O_2(el))} \cdot \left\{ F(O_2(el)) + \frac{\varphi(\,^5\pi_g \rightarrow el)\cdot F\left(O_2(\,^5\pi_g)\right)}{1+\frac{[O]\cdot k\left(O_2(\,^5\pi_g);O\right)}{[O_2]\cdot k\left(O_2(\,^5\pi_g);O_2\right)}} \right\} \tag{7}$$

where $Q(O_2(el))$ is a quenching factor of the $O_2(el)$ (see below). The first term in brackets corresponds to the one-stage (direct) process of $O_2(el)$ excitation, the second term is a two-stage mechanism considering the reaction (6).

The Barth's mechanism is also a non-alternative source of excitation of the $O(^1S)$ in the nighttime lower thermosphere (below 105 km). However, the actual precursor of $O(^1S)$ excitation remains a matter of debate (Witt et al., 1979; McDade et al., 1986; Bates, 1992; Mende et al., 1993). The energy transfer from the precursor to the $O$ ($^1$S) (threshold of excitation 4.19 eV) occurs according to a two-stage scheme

$$[O(\,^1S)] = \frac{[O]^2[M]\cdot k(O;O;M)}{Q(O(\,^1S))} \cdot \frac{\varphi(precursor \rightarrow S)\cdot F(O_2(precursor))}{1+\frac{[O_2]\cdot k(O_2(precursor);O_2)}{[O]\cdot k(O_2(precursor);O)}} \tag{8}$$

where $\varphi(precursor \rightarrow S)$ is the quantum yield of $O(^1S)$ production in the quenching reaction of the precursor with oxygen atom

$$O_2(precursor)+O(\,^3P) \rightarrow O_2+O(*) \tag{9}$$

where (*) denotes any excited state.

In ((7) and (8)), there are three types of parameters depending on temperature. We have already discussed two of them, $k(O;O;M)$ and $F(O_2(el))$. The third parameter is the quenching factor equal to

$$Q(O_2(el)) = \tau_{el}^{-1} + [O_2]\cdot k(O_2(el);O_2) + [O]\cdot k(O_2(el);O) + [N_2]\cdot k(O_2(el);N_2) \text{ or}$$

$$Q\left(O(\,^1S)\right) = \tau_S^{-1} + [O_2]\cdot k\left(O(\,^1S);O_2\right) + [O] \cdot k\left(O(\,^1S);O\right) + [N_2]\cdot k\left(O(\,^1S);N_2\right) \tag{10}$$

In (10), $\tau$ is the radiative lifetime of the excited component, $k(*;y)$ denotes rate coefficient of a reaction involving excited component * and collisional partner y ($O_2$, $N_2$ and $O(^3P)$). As we showed in (Yankovsky and Manuilova, 2018), collisions with other atmospheric components in the altitude range of 80–120 km are not effective.

## 3. Sensitivity study

The results of calculations by the Barth's mechanism depend on temperature, since the three-body reaction of recombination of oxygen atoms, quantum yields of the formation of electronic states of the oxygen molecule, and even the reactions of quenching of these states depend on temperature. The sensitivity analysis makes it possible to obtain an integral temperature dependence considering all these factors.

The sensitivity coefficient responsible for the dependence of the concentration of the excited component on the gas temperature (see Yankovsky et al., 2016) is

$$S(O_2(el);T) = \frac{T}{[O_2(el)]} \cdot \frac{\partial [O_2(el)]}{\partial T} \tag{11}$$

The dimensionless sensitivity coefficient in the form of the logarithmic derivative (11) has an evident physical meaning. Namely, the exponent factor in expression (12) characterizes the dependence of concentration on temperature:

$$[O_2(el)] \propto (T)^{S(O_2(el);T)} \tag{12}$$

To demonstrate the capabilities of this approach, we first construct the sensitivity coefficient for the two-channel Barth's mechanism without considering the temperature dependence of the quenching factor. Using the definition (11) and the solution of balance equation (7) we obtain (Yankovsky, 2020):

$$S(O_2(el);T) = \frac{\left\{ \left(\frac{T}{\vartheta_{el}} - 2\right) \cdot F(O_2(el)) + \frac{\varphi(\ ^5\pi_g \to el) \cdot F\left(O_2(\ ^5\pi_g)\right)}{1 + \frac{[O] \cdot k(O_2(\ ^5\pi_g);O)}{[O_2] \cdot k(O_2(\ ^5\pi_g);O_2)}} \cdot \left(\frac{T}{\vartheta_{5\pi}} - 2\right) \right\}}{F(O_2(el)) + \frac{\varphi(\ ^5\pi_g \to el) \cdot F\left(O_2(\ ^5\pi_g)\right)}{1 + \frac{[O] \cdot k(O_2(\ ^5\pi_g);O)}{[O_2] \cdot k(O_2(\ ^5\pi_g);O_2)}}} \tag{13}$$

Formula (13) is correct for the temperature range of 140–370 K (see above).

If the quantum yield of the precursors were independent of temperature (all values of $\theta_{el}$ from Table 1 tend to infinity), we would get an obvious result from (13), namely, $S(O_2(el);T) = -2$. The temperature coefficient of the three-body reaction of the recombination of oxygen atoms (1) has just such a temperature dependence. We consider the impact the quenching factor on the sensitivity coefficient (13) for the three most famous atmospheric experiments in the next section.

## 4. Discussion

Using the obtained theoretical expressions, an analysis of the experimental data obtained *in situ* and simultaneously during the rocket experiments ETON, MULTIFOT92, WADIS-2 was carried out. In each of these experiments, the Barth's mechanism was used to theoretically interpret the experimental data.

### 4.1. Mechanism of $O_2(A^3\Sigma_u^+, v)$ production in the ETON and MULTIFOT92 experiments.

The authors of these experiments concluded that altitude profile of VER in Herzberg 1 band was formed as result of a one-stage channel of the Barth's mechanism (Thomas et al., 1979; Thomas, 1981; Thomas and Young, 1981; McDade et al., 1986; Melo et al., 1997). For reaction of the $O_2(A^3\Sigma_u^+, v = 0-5)$ quenching in collisions with $O_2$, $N_2$, $O(^3P)$ the temperature dependence has not yet been found (see Table A1 in Appendix). Therefore, following (13), we obtain the sensitivity coefficient for the $O_2(A^3\Sigma_u^+, v)$ production in the Barth's one-stage mechanism from (7) in form:

$$S(O_2(A^3\Sigma);T) = \frac{T}{\theta_{A3\Sigma}} - 2 \tag{14}$$

The dependence of $[O_2(A^3\Sigma_u^+, v)]$ on temperature (14) is of the order of $(T)^{-1}$ in the altitude range from 85 to 110 km (Fig. 3, line **b**). Small variations of sensitivity coefficient, $S(O_2(A^3\Sigma);T)$, depending on altitude are naturally related to the variability of the temperature profile.

### 4.2. Mechanism of $O(^1S)$ production in the ETON and MULTIFOT92 experiments.

We supplemented the mechanism with measurement of the rate coefficient of reaction $O(^1S) + O_2 \to products$, having a strong 'negative' dependence on temperature:

$$k(O(^1S);O_2) = A_{S;O2} exp\left(\frac{b_{S;O2} + \beta_{S;O2} \cdot T^2}{T}\right) \tag{15}$$

where $A_{S;O2} = 2.32 \cdot 10^{-12}$ cm$^3$ s$^{-1}$, $b_{S;O2} = -812$ K, $\beta_{S;O2} = 1.82 \cdot 10^{-3}$ K$^{-1}$ for temperature in range of 215–473 K (see Table A1 in Appendix). The rate coefficients, $k(O(^1S);O(^3P))$ and $k(O(^1S);N_2)$, do not depend on temperature (see Slanger and Black, 1981). In accordance with definition (11) sensitivity coefficients for the $O(^1S)$ production in the Barth's two-stage mechanism from (8) is

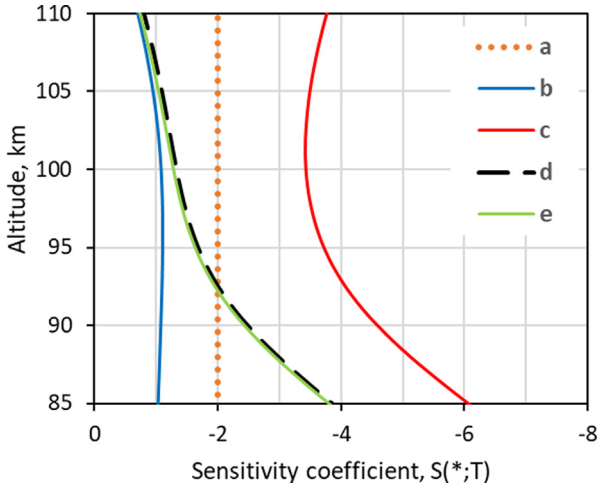


Fig. 3. Sensitivity to the temperature of the volume emission rates from two excited oxygen components at night. Only the temperature dependence of the three-body reaction of recombination of oxygen atoms (1) is used in case **a**. In other cases, the temperature dependencies for the quantum yields of precursors and quenching factors were also considered. Line **b** – $O_2\left(A^3\Sigma_u^+\right)$ from direct one-stage reaction (1), see (14). For $O(\ ^1S)$ we consider three types of precursor: **c** – $O_2(\ ^5\pi_g)$, **d** – $O_2\left(A^3\Sigma_u^+\right)$, **e** – $O_2\left(A'^3\Delta_u\right)$, respectively.

$$S\left(O(\ ^1S);T\right)=\frac{T}{\theta_{precursor}}-2+\frac{[O_2]\cdot k(O(\ ^1S);O_2)}{Q(O(\ ^1S))}\cdot\left(\frac{b_{S;O2}}{T}-T\cdot\beta_{S;O2}\right) \tag{16}$$

The sensitivity analysis (16) shows a strong dependence of $[O(^1\mathrm{S})]$ on temperature fluctuations. Values of $S(O(^1\mathrm{S});T)$ may take values between −1 and −5 (Fig. 3, lines **c**, **d**, **e**). This effect is most noticeable for the precursor $O_2(^5\pi_g)$ (see Fig. 3, line **c**), but if the precursor of the green line emission is $O_2\left(A^3\Sigma_u^+,v\right)$ or $O_2\left(A'^3\Delta_u,v\right)$ then the sensitivity coefficient $S(O(^1S);T)$ lies in the range from −1 to −3 (lines **d** and **e** in Fig. 3) in the altitude range of 92–105 km, where the Barth's mechanism is the actual source of the green line emission. At lower altitudes (below 92 km), the sensitivity of the green line intensity to temperature is controlled mainly by the collisional quenching (see the last term on the right side of expression (16)).

Thus, the analysis of sensitivity to temperature opens the possibility of solving the problem of defining the $O(^1S)$ precursor in the nightglow. An abnormally strong dependence of the intensity variations of the green line of atomic oxygen on fluctuations of temperature (the values of $S(O(^1S);T)$ less than −3 in the altitude range of 92–105 km) can be provided only by the precursor $O_2(^5\pi_g)$. If $S(O(^1S);T)$ takes a value greater than −2, then $O_2(^5\pi_g)$ is obviously not a precursor. The main requirement to determine the $O(^1S)$ precursor is that fluctuations of $[O(^1S)]$ and temperature must be measured simultaneously and *in situ*.

### 4.3. Sensitivity of $O_2\left(b^1\Sigma_g^+\right)$ production to temperature

This is the most difficult case compared to those considered earlier. We need to consider all the declared factors affecting the sensitivity to temperature. This excited state of $O_2$ is populated both in a one-stage and a two-stage Barth's mechanism, in addition, the quenching factor also depends on temperature.

This problem has a long history. In 1978, Noxon (1978) reported numerous observations of simultaneous large quasiperiodic fluctuations in the rotational temperature and the intensity of the $O_2$ Atmospheric band in nightglow. He also noted that there was evidence of similar variations in the Doppler temperature and intensity of the green line of oxygen in approximately the same range of atmospheric heights (about 95 km). Noxon (1978) emphasizes that temperature (and wind) fluctuations are an immediate reaction of the atmosphere in the presence of a gravity wave. At the same time, the reaction of the intensity of nightglow is much less direct, since it includes the behavior of chemical reactions involving excited components of the atmosphere depending on the gas temperature. The fluctuations in temperature and radiation intensities are such that they should be taken into account in all mesospheric chemical theories where there are reactions, the rate coefficients of which depends on temperature (Noxon, 1978).

In this section, we deal with this very task. We carried out a numerical experiment to determine the sensitivity coefficient $O_2(\mathrm{b}^1\Sigma_\mathrm{g}^+)$ to temperature and its precursor based on publicly available results of rocket experiments.

#### 4.3.1. Analytical expression for sensitivity coefficient, $S\left(O_2\left(b^1\Sigma\right);T\right)$

Following ((11) and (13)) we obtain the sensitivity coefficient of $O_2\left(b^1\Sigma_g^+\right)$ to temperature:

$$S\left(O_2\left(b^1\Sigma\right);T\right)=\frac{\left\{\left(\frac{T}{\vartheta_{b1\Sigma}}-2\right)\cdot F\left(O_2\left(b^1\Sigma\right)\right)+\frac{\varphi(precursor\to b^1\Sigma)\cdot F(precursor)}{1+\frac{[O]\cdot k(O_2(precursor);O)}{[O_2]\cdot k(O_2(precursor);O_2)}}\cdot\left(\frac{T}{\theta_{precursor}}-2\right)\right\}}{F\left(O_2\left(b^1\Sigma\right)\right)+\frac{\varphi(precursor\to b^1\Sigma)\cdot F(precursor)}{1+\frac{[O]\cdot k(O_2(precursor);O)}{[O_2]\cdot k(O_2(precursor);O_2)}}}+\frac{[N_2]\cdot k\left(O_2\left(b^1\Sigma\right);N_2\right)}{Q\left(O_2\left(b^1\Sigma\right)\right)}\cdot\left(\frac{b_{b;N2}}{T}\right) \tag{17}$$

The last term on right side of expression (16) shows the sensitivity of $[O_2(b^1\Sigma_g^+)]$ to temperature due to its

Table 2
The values of $F(O_2(^5\pi_g)) \cdot \varphi(^5\pi_g \rightarrow b^1\Sigma_g^+)$ and $k(O_2(^5\pi_g);O)/k(O_2(^5\pi_g);O_2)$ parameter sets used for sensitivity study of $[O_2(b^1\Sigma_g^+)]$ to temperature fluctuations.

| Experiment | ETON (McDade et al., 1986) | WADIS-2 (Grygalashvyly et al., 2019) |
|---|---|---|
| Altitude profile of $[O(^3P)]$ from | MSIS for ETON | MSIS for WADIS-2 |
| $\varphi(\ ^5\pi_g \rightarrow b^1\Sigma_g^+) \cdot F(O_2(\ ^5\pi_g))$ | $0.15 \pm 0.01$ | $0.08^{+0.12}_{-0.04}$ |
| $k(O_2(\ ^5\pi_g);O)/k(O_2(\ ^5\pi_g);O_2)$ | $2.9 \pm 0.5$ | $0.23^{+0.36}_{-0.14}$ |

quenching factor. The rate coefficient of the reaction $O_2(b^1\Sigma_g^+) + N_2 \rightarrow products$ is

$$k\left(O_2\left(b^1\Sigma\right);N_2\right) = A_{b;N2} \cdot \exp\left(\frac{b_{b;N2}}{T}\right) \quad (18)$$

where $A_{b;N2} = 2.03 \cdot 10^{-15}$ cm$^3$ s$^{-1}$, $b_{b;N2} = 37$ K for $T =$ 210–370 K (see Table A1 in Appendix). The rate coefficients $k(O_2(b^1\Sigma);O(^3P))$ and $k(O_2(b^1\Sigma);O_2)$ do not depend on temperature (see Burkholder et al., 2015).

Following the point of view of most researchers on the mechanism of formation of $O_2(b^1\Sigma_g^+)$ molecules in nightglow, we believe that its precursor in the Barth's mechanism is the $O_2(^5\pi_g)$ state. Below we discuss three other precursors: $O_2\left(A^3\Sigma_u^+\right)$, $O_2\left(A'^3\Delta_u\right)$, $O_2\left(c^1\Sigma_u^-\right)$.

The values of quantum yield of $O_2(b^1\Sigma_g^+)$ in reaction (6), $\varphi(^5\pi_g \rightarrow b^1\Sigma_g^+)$, rate coefficients of quenching of the precursor $O_2(\ ^5\pi_g)$ in collisions with $O(^3P)$ and $O_2$, $k(O_2(^5\pi_g);O)$ and $k(O_2(^5\pi_g);O_2)$, from (17), are not known until now. However, two expressions, $k(O_2(^5\pi_g);O)/k(O_2(^5\pi_g);O_2)$ and $\varphi(^5\pi_g \rightarrow b^1\Sigma_g^+) \cdot F(O_2(^5\pi_g))$, involving these parameters can be measured according to the technique proposed in (McDade et al., 1986). The values of these constants obtained in rocket experiments ETON (McDade et al., 1986) and WADIS-2 (Grygalashvyly et al., 2019) are presented in Table 2. Note that the results of the MULTIFOT92 experiment (Takahashi et al., 1996) were close to ETON.

At first glance, ETON and WADIS-2 data sets from Table 2 are not consistent. However, we consider the temperature dependence of the quantum yield of the precursor $F(O_2(^5\pi_g))$, as was done above (Section 1). In (Grygalashvyly et al., 2019), the parameters were determined for the altitude range of 92–103 km, and in the middle of this interval, a wide local peak of gas temperature about 205 K (see Fig. 1a in Grygalashvyly et al., 2019) was recorded in the experiment. At this temperature, the value of $F(O_2(^5\pi_g)) \cong 0.60$ (see Fig. 1). Therefore, we obtain an estimate for the quantity $\varphi(^5\pi_g \rightarrow b^1\Sigma_g^+) \cong 0.13$ (see the first line in Table 3). In the ETON experiment (McDade et al., 1986), it was not possible to measure the altitude temperature profile at the same time *in situ*, so we can only rely on the temperature profile from MSIS for this event. The Barth's mechanism parameters were determined for an altitude range of approximately 90–110 km. In the middle of this interval there is a local gas temperature minimum of 170–175 K, following the MSIS model. The value of $F(O_2(^5\pi_g))$ reaches a value of 0.75 at these temperatures (Fig. 1). Then we get an estimate of $\varphi(^5\pi_g \rightarrow b^1\Sigma_g^+) \cong 0.2$ (Table 3), but with an uncertainty factor of at least 1.5 since the temperature profile is not experimentally measured.

Table 3
The values of $O_2(b^1\Sigma_g^+)$ quantum yield, $\varphi(\text{precursor} \rightarrow b^1\Sigma_g^+)$, calculated in this work from experimental data for various proposed precursors of the Barth's mechanism.

| Precursor | $\varphi\left(precursor \rightarrow b^1\Sigma_g^+\right)$ | |
|---|---|---|
| | Experiment ETON | Experiment WADIS-2 |
| $O_2(\ ^5\pi_g)$ | $0.2 \pm 0.1$ | $0.13^{+0.20}_{-0.06}$ |
| $O_2\left(A^3\Sigma_u^+\right)$ | 6.1 | 2.7 |
| $O_2\left(A'^3\Delta_u\right)$ | 1.6 | 0.8 |
| $O_2\left(c^1\Sigma_u^-\right)$ | 6.0 | 3.0 |

As can be seen from Table 3, according to our estimates, both sets of constants for the Barth's mechanism (McDade et al., 1986; Grygalashvyly et al., 2019) give almost identical values of the quantum yield $\varphi(^5\pi_g \rightarrow b^1\Sigma_g^+)$ taking into account uncertainties. A more accurate determination of this value is possible only based on a new experiment *in situ*.

#### 4.3.2. Numerical experiment for determination of $O_2\left(b^1\Sigma_g^+\right)$ precursor

The data sets of the parameters of the Barth's mechanism, measured experimentally (Table 2), are quite sufficient to deal with the type of precursor of the emission of the molecule in nightglow. We carried out a numerical experiment, calculating the sensitivity coefficient, $S(O_2(b^1\Sigma);\ T)$, for 9 model scenarios, which are presented in Table 4 (see Fig. 4). The $S(O_2(b^1\Sigma);\ T)$ altitude profiles were calculated according to the formula (17) in which not only the $O_2(\ ^5\pi_g)$state, but also three others states, $O_2\left(A^3\Sigma_u^+\right)$, $O_2\left(A'^3\Delta_u\right)$, $O_2\left(c^1\Sigma_u^-\right)$, were used as a precursor. Also, for all precursors, estimates of the quantum yield of $O_2(b^1\Sigma)$ molecules (as in Section 4.3.1) were provided, ensuring agreement with the measured sets of constants from the experiments (Table 2). The results of these estimates show that only the precursor $O_2(\ ^5\pi_g)$can provide the observed $O_2(b^1\Sigma)$ concentrations in the nightglow. We are forced to reject the other precursors, since, to agree with the experiment, they must form $O_2(b^1\Sigma)$ molecules with a "physically" impossible quantum yield greater than 1 (see Table 3).

Another confirmation that both sets of parameters for the Barth's mechanism (ETON and WADIS-2) do not contradict each other is shown in Fig. 4. The coefficients of

Table 4
Scenarios of the numerical experiments for calculations of sensitivity coefficient, $S(O_2(b^1\Sigma); T)$, which used in Fig. 4.

| Experiment | Parameter's set (see Table 2) | Precursor | Index in Fig. 4 |
|---|---|---|---|
| Temperature dependence of the three-body recombination of oxygen atoms, Eq. (1) | | | ***a*** |
| ETON | McDade et al. (1986) | $O_2(^5\pi)$ | ***f*** |
| ETON | McDade et al. (1986) | $O_2(A^3\Sigma; A'^3\Delta; c^1\Sigma)$ | ***g*** |
| ETON | Grygalashvyly et al. (2019) | $O_2(^5\pi)$ | ***h*** |
| ETON | Grygalashvyly et al. (2019) | $O_2(A^3\Sigma; A'^3\Delta; c^1\Sigma)$ | ***i*** |
| WADIS2 | Grygalashvyly et al. (2019) | $O_2(^5\pi)$ | ***j*** |
| WADIS2 | Grygalashvyly et al. (2019) | $O_2(A^3\Sigma; A'^3\Delta; c^1\Sigma)$ | ***k*** |
| WADIS2 | McDade et al. (1986) | $O_2(^5\pi)$ | ***l*** |
| WADIS2 | McDade et al. (1986) | $O_2(A^3\Sigma; A'^3\Delta; c^1\Sigma)$ | ***m*** |

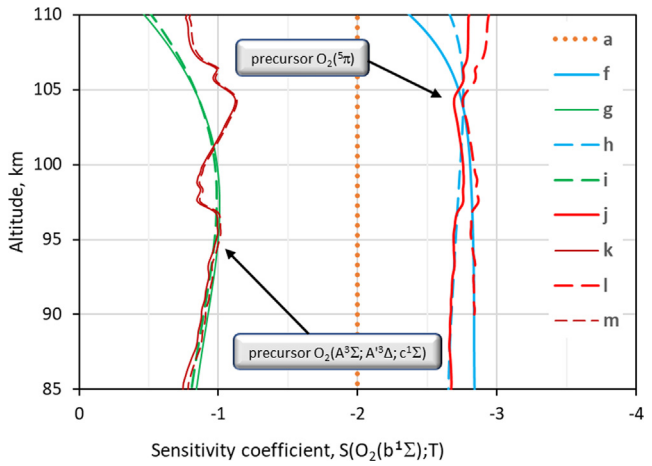


Fig. 4. Sensitivity of the volume emission rate from $O_2(b^1\Sigma_g^+)$ molecule to temperature in the nightglow. Nine cases are under consideration: see notation in Table 4 and text.

sensitivity $[O_2(b^1\Sigma_g^+)]$ to temperature calculated for the conditions of two experiments (ETON and WADIS-2) using two alternative sets of Barth's mechanism constants (Table 2) give very close values in a comparable altitude range of 92–105 km (Fig. 4, lines ***f***, ***h***, ***j*** and ***l***). This result was obtained considering the temperature dependence of not only the rate coefficient of the reaction (1), but also considering the temperature dependence of the quantum yields of the reaction products. The discrepancies between the results of modeling the sensitivity coefficient at altitudes above 105 km are associated more with the uncertainties in the altitude profile of atomic oxygen, but this is not the subject of this study. If we take into account the temperature dependence of the quantum yields of the precursor in reaction (1), then the concentration of $O_2\left(b^1\Sigma_g^+\right)$ in the altitude range of 85–110 km (Fig. 4, lines ***f***, ***h***, ***j*** and ***l***) depends more strongly on temperature than if the concentration depended only on the reaction of recombination of oxygen atoms (see Fig. 4, line **a**). Approximately this relationship can be described as $[O_2(b^1\Sigma_g^+)] \propto (T)^{-2.8}$ in altitude range of 92–105 km.

## 5. Summary

In this study, the effect of atmospheric temperature on calculation the intensity of oxygen emissions in the framework of the Barth's mechanism is investigated. The calculations have been performed based on sensitivity analysis. The temperature dependence of the processes of excitation and quenching for excited components such as $O(^1S)$, $O_2(b^1\Sigma_g^+)$, $O_2(A^3\Sigma_u^+)$ is considered for the altitude interval of 85–110 km. The results show that the analysis proposed in this study might be used in order to determine (i) a type of $O(^1S)$ precursor (Section 4.2) and (ii) quantum yield of $O_2\left(b^1\Sigma_g^+\right)$ as a result of the collisional reaction of the precursor with $O_2$ (Section 4.3.1). Available experimental data led to the conclusion that the $O_2(\ ^5\pi_g)$ state is a precursor of $O_2(b^1\Sigma_g^+)$ in the Barth's mechanism (Section 4.3.2). The analytical formulas obtained are also suitable for estimating the temperature effect on the contribution of the Barth's mechanism to atmospheric dayglow. However, further investigations are necessary.

## 6. Data availability

Data of MSIS-E-90 Atmosphere Model are available via https://ccmc.gsfc.nasa.gov/modelweb/models/msis_vitmo.php (last accessed 6 June 2020).

WADIS-2 data are available via the IAP ftp server at ftp://ftp.iap-kborn.de/data-in-publications/GrygalashvylyACP2018 (last access: 25 November 2019).

Data of TIMED-SABER—Sounding of the Atmosphere Using Broadband Emission Radiometry. Available online: http: //saber.gats-inc.com/data.php (accessed on 19 January 2020).

## Declaration of Competing Interest

The authors declare that they have no known competing financial interests or personal relationships that could have appeared to influence the work reported in this paper.

## Acknowledgments

The author is grateful to Ekaterina Vorobeva for a thorough discussion of all aspects of the work. Also, the author is thankful to two anonymous reviewers for valuable comments. This work was supported by the Russian Foundation for Basic Research (RFBR grant No. 20-05-00450 A). The author dedicates this work to the memory of his teacher, Prof. Gustav Shved (1936–2020).

## Appendix A.

### *A.1. Altitude profiles of the gas temperature in the upper mesosphere and lower thermosphere*

Barth's mechanism is usually used to interpret measurements of oxygen emission intensities in the altitude interval of 85–110 km (Witt et al., 1979; Thomas, 1981; McDade et al., 1986; Mende et al., 1993; Melo et al., 1997; Grygalashvyly et al., 2019, etc.). The gas temperature profiles shown in these works were extremely diverse, especially in those cases when it was actually possible to measure them. To clarify the range of possible temperature variations, we considered an extended range of altitudes and used the database obtained in the TIMED-SABER experiment for 2003–2019. For example, Fig. A1 shows a selection of $T_k$ altitude profiles for one day in accordance with satellite data in a wide range of values of Solar Zenith Angle, SZA = 68–105° and Latitude = 35–75 N. Based on selected events, we analyzed the effect of temperature within the Barth's mechanism in the range of 140–370 Kelvin (see Section 1).

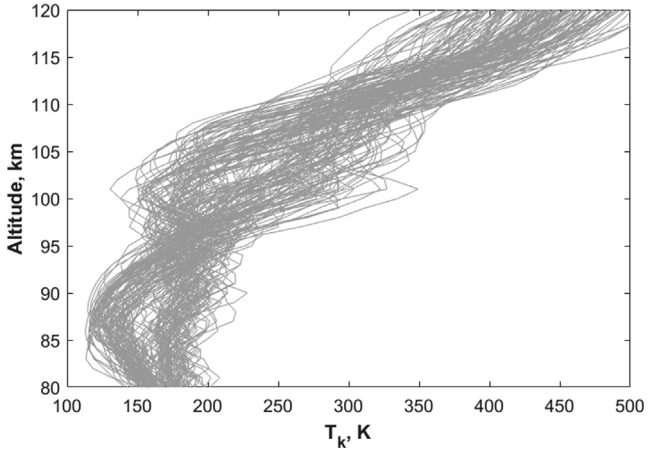


Fig. A1. The profiles of gas kinetic temperature from TIMED-SABER data for 2010 22 June, 90 random events, Latitude = 35–75 N, SZA (Solar Zenith Angle) = 68–105°.

### *A.2. A complete list of values of the Einstein coefficients and the reaction rate coefficients (together with the uncertainties) used in the work is presented in Table A1*

See Table A1.

Table A1
Laboratory quenching rate coefficients, $k(*;Q)$, and radiative lifetimes, τ, for excited components, where * denotes $O(^1S)$, $O_2\left(b^1\Sigma_g^+, v=0\right)$, $O_2(A^3\Sigma_u^+, v=0-5)$. Values of $k(*;Q)$ are given taking into account the dependence on temperature (where RT is the room temperature in the range of 290–300 K) for collisional partner, $Q$: $O_2$, $O(^3P)$ and $N_2$. Status for September 2020.

| Process | Parameter | Value of parameter | Temperature range | References |
|---|---|---|---|---|
| $O(^1S) \rightarrow O(^1D)$ and $O(^3P) + hv$ | $\tau_S$ | 0.74 s | | McDade et al. (1986) |
| $O(^1S) + O_2 \rightarrow$ products | $k(O(^1S);O_2)$ | $A_{S;O2}exp\left(\frac{b_{S;O2}+\beta_{S;O2}\cdot T^2}{T}\right)$, *where* $A_{S;O2} = (2.32 \pm 0.94)\cdot 10^{-12}$ cm$^3$ s$^{-1}$, $b_{S;O2} = -(812 \pm 130)K$, $\beta_{S;O2} = (1.82 \pm 0.95)\cdot 10^{-3}$ K$^{-1}$ | T = 215–473 K | Capetanakis et al. (1993) |
| $O(^1S) + O(^3P) \rightarrow$ products | $k(O(^1S);O(^3P))$ | $2\cdot 10^{-14}$ cm$^3$ s$^{-1}$ | RT | Slanger and Black (1981) |
| $O(^1S) + N_2 \rightarrow$ products | $k(O(^1S);N_2)$ | $<5\cdot 10^{-17}$ cm$^3$ s$^{-1}$ | RT | |
| $O_2\left(b^1\Sigma_g^+, v=0\right) \rightarrow O_2\left(X^3\Sigma_g^-, v'\right)$ *and* $O_2\left(a^1\Delta_g, v''\right) + hv$ | $\tau_b$ | 11.0 s | | Yankovsky et al. (2019) |
| $O_2\left(b^1\Sigma_g^+, v=0\right) + O_2 \rightarrow$ *products* | $k(O_2(b);O_2)$ | $(3.9 \pm 2.0)\cdot 10^{-17}$ cm$^3$ s$^{-1}$ | RT | Burkholder et al. (2015) |
| $O_2\left(b^1\Sigma_g^+, v=0\right) + O(^3P) \rightarrow$ *products* | $k(O_2(b);O(^3P))$ | $8\cdot 10^{-14}$ cm$^3$ s$^{-1}$, relative uncertainty $\Delta k/k = 4$ | RT | |
| $O_2\left(b^1\Sigma_g^+, v=0\right) + N_2 \rightarrow$ *products* | $k(O_2(b);N_2)$ | $A_{b;N2}exp\left(\frac{b_{b;N2}}{T}\right)$, *where* $A_{b;N2} = (2.03 \pm 0.30)\cdot 10^{-15}$ cm$^3$ s$^{-1}$ $b_{b;N2} = (37 \pm 40)K$ | T = 210–370 K | Dunlea et al. (2005) |
| $O_2(A^3\Sigma_u^+, v)^a \rightarrow O_2\left(X^3\Sigma_g^-, v'\right) + hv$ | $\tau_{A,v}$ | 0.095 s | | Bates (1989) |
| $O_2(A^3\Sigma_u^+, v)^a + O_2 \rightarrow$ *products* | $k(O_2(A,v);O_2)$ | $(2.9 \pm 2.0)\cdot 10^{-13}$ cm$^3$ s$^{-1}$ | RT | Kenner and Ogryzlo (1984), Knutsen et al. (1994) |
| $O_2(A^3\Sigma_u^+, v)^a + O(^3P) \rightarrow$ *products* | $k(O_2(A,v);O(^3P))$ | $(1.3 \pm 0.2)\cdot 10^{-11}$ cm$^3$ s$^{-1}$ | RT | Knutsen et al. (1994) |
| $O_2(A^3\Sigma_u^+, v)^a + N_2 \rightarrow$ *products* | $k(O_2(A,v);N_2)$ | $(9.3 \pm 1.7)\cdot 10^{-15}$ cm$^3$ s$^{-1}$ | RT | |

[a] – the value of the parameter is true for v = 0–5.

## References


Bates, D.R., 1988. Excitation and quenching of the oxygen bands in the nightglow. Planet. Space Sci. 36 (9), 875–881. https://doi.org/10.1016/0032-0633(88)90093-1.

Bates, D.R., 1989. Oxygen band system transition arrays. Planet. Space Sci. 37 (7), 831–837. https://doi.org/10.1016/0032-0633(89)90139-6.

Bates, D.R., 1992. Nightglow emissions from oxygen in the lower thermosphere. Planet. Space Sci. 40 (2/3), 211–221. https://doi.org/10.1016/0032-0633(92)90059-W.

Burkholder, J.B., Abbatt, J.P.D., Huie, R.E., Kurylo, M.J., Wilmouth, D. M., Sander, S.P., Barker, J.R., Kolb, C. E., Orkin, V.L., Wine, P.H., 2015. Chemical Kinetics and Photochemical Data for Use in Atmospheric Studies. JPL Publication 15-10, Evaluation Number 18, California Institute of Technology, Pasadena, California. http://hdl.handle.net/2014/45510.

Campbell, I.M., Gray, C.N., 1973. Rate constants for $O(^3P)$ recombination and association with $N(^4S)$. Chem. Phys. Lett. 18 (4), 607–609. https://doi.org/10.1016/0009-2614(73)80479-8.

Capetanakis, F.P., Sondermann, F., Hoser, S., Stuhl, F., 1993. Temperature dependence of the quenching of $O(^1S)$ by simple inorganic molecules. J. Chem. Phys. 98 (10), 7883–7887. https://doi.org/10.1063/1.464596.

Dunlea, E.J., Talukdar, R.K., Ravishankara, A.R., 2005. Kinetics studies of the reactions of $O_2(b^1\Sigma)$ with several atmospheric molecules. J. Phys. Chem. 109 (A17), 3912–3920. https://doi.org/10.1021/jp044129x.

Grygalashvyly, M., Eberhart, M., Hedin, J., Strelnikov, B., Lübken, F.-J., Rapp, M., Lohle, S., Fasoulas, S., Khaplanov, M., Gumbel, J., Vorobeva, E., 2019. Atmospheric band fitting coefficients derived from a self-consistent rocket-borne experiment. Atmos. Chem. Phys. 19, 1207–1220. https://doi.org/10.5194/acp-19-1207-2019.

Kenner, R.D., Ogryzlo, E.A., 1984. Quenching of the O2(Av=2 → Xv=5) Herzberg I band by O2(a) and O. Canadian Journal of Physics 62 (12), 1599–1602.

Klotz, R., Peyerimhoff, S.D., 1986. Theoretical study of the intensity of the spin- or dipole forbidden transitions between the $c^1\Sigma$, $A'^3\Delta$, $A^3\Sigma$ and $X^3\Sigma$, $a^1\Delta$, $b^1\Sigma$ states in $O_2$. Mol. Phys. 57 (3), 573–594. https://doi.org/10.1080/00268978600100421.

Knutsen, K., Dyer, M.J., Copeland, R.A., 1994. Laser double-resonance study of the collisional removal of $O_2(A^3\Sigma, v=6, 7$ and 9) with $O_2$, $N_2$, $CO_2$, Ar and He. J. Chem. Phys. 101 (9), 7415–7422. https://doi.org/10.1063/1.468418.

Krasnopolsky, V.A., 2011. Excitation of the oxygen nightglow on the terrestrial planets. Planet. Space Sci. 59 (8), 754–766. https://doi.org/10.1016/j.pss.2011.02.015.

Krasnopolsky, V. A., 1987. Fizika svecheniya atmosfer planet I komet (Physics of Atmospheric Emissions for Planets and Comets), Moscow: Nauka, 304, pp. 1987.

Krupenie, P.H., 1972. The spectrum of molecular oxygen. J. Phys. Chem. Ref. Data 1 (2), 423–521. https://doi.org/10.1063/1.3253101.

Lednyts'kyy, O., von Savigny, C., 2020. Photochemical modelling of molecular and atomic oxygen based on multiple nightglow emissions measured in situ during the Energy Transfer in the Oxygen Nightglow rocket campaign. Atmos. Chem. Phys. 20, 2221–2261.

McDade, I.C., Murtagh, D.P., Greer, R.G.H., Dickinson, P.H.G., Witt, G., Stegman, J., Llewellyn, E.J., Thomas, L., Jenkins, D.B., 1986. ETON 2: quenching parameters for the proposed precursor of $O_2(b^1\Sigma)$ and $O(^1S)$ in the terrestrial nightglow. Planet. Space Sci. 34 (9), 789–800. https://doi.org/10.1016/0032-0633(86)90075-9.

Melo, S.M.L., Takahashi, H., Clemesha, B.R., Stegman, J., 1997. The $O_2$ Herzberg I bands in the equatorial nightglow. J. Atmos. Sol. Terr. Phys. 59 (3), 295–304. https://doi.org/10.1016/S1364-6826(96)00038-7.

Mende, S.B., Swenson, G.R., Geller, S.P., Viereck, R.A., Murad, E., Pike, C.P., 1993. Limb view spectrum of the Earth's airglow. J. Geophys. Res. A 98 (A11), 19117–19125. https://doi.org/10.1029/93JA02282.

Murtagh, D.P., Witt, G., Stegman, J., McDade, I.C., Llewellyn, E.J., Harris, F., Greer, R.G.H., 1990. An assessment of proposed $O(^1S)$ and $O_2(b^1\Sigma)$ nightglow excitation parameters. Planet. Space Sci. 38 (1), 43–53. https://doi.org/10.1016/0032-0633(90)90004-A.

Noxon, J.F., 1978. Effect of internal gravity waves upon night airglow temperatures. Geophys. Res. Lett. 5 (1), 25–27. https://doi.org/10.1029/GL005i001p00025.

Partridge, H., Bauschlicher, C.W., Langhoff, S.R., Taylor, P.R., 1991. Theoretical study of low-lying bound states of $O_2$. J. Chem. Phys. 95 (11), 8292–8300. https://doi.org/10.1063/1.461309.

Saxon, R.P., Liu, B., 1977. Ab initio configuration interaction study of the valence states of $O_2$. J. Chem. Phys. 67 (12), 5432–5441. https://doi.org/10.1063/1.434764.

Slanger, T.G., Black, G., 1981. Quenching $O(^1S)$ by $O_2(a^1\Delta)$. Geophys. Res. Lett. 8 (5), 535–538. https://doi.org/10.1029/GL008i005p00535.

Takahashi, H., Clemesha, B.R., Simonich, D.M., Melo, S.M.L., Teixeira, N.R., Eras, A., Stegman, J., Witt, G., 1996. Rocket measurements of equatorial airglow: MULTIFOT92 database. J. Atmos. Terr. Phys. 58 (16), 1943–1961. https://doi.org/10.1016/0021-9169(95)00158-1.

Thomas, L., Greer, R.G.H., Dickinson, P.G.H., 1979. The excitation of the 557.7 nm line and Herzberg bands in the nightglow. Planet. Space Sci. 27, 925–931. https://doi.org/10.1016/0032-0633(79)90022-9.

Thomas, R.J., 1981. Analyses of atomic oxygen, the green line, and Herzberg bands in the lower thermosphere. J. Geophys. Res. 86 (A1), 206–210. https://doi.org/10.1029/JA086iA01p00206.

Thomas, R.J., Young, R.A., 1981. Measurement of atomic oxygen and related airglows in the lower thermosphere. J. Geophys. Res. 86 (C8), 7389–7393. https://doi.org/10.1029/JC086iC08p07389.

Witt, G., Stegman, J., Solheim, B.H., Llewellyn, E.J., 1979. A measurement of the $O_2(b^1\Sigma - X^3\Sigma)$ Atmospheric Band and the $O(^1S)$ green line in the nightglow. Planet. Space Sci. 27, 341–350. https://doi.org/10.1016/0032-0633(79)90111-9.

Wraight, P.C., 1982. Association of atomic oxygen and airglow excitation mechanisms. Planet. Space Sci. 30 (3), 251–259. https://doi.org/10.1016/0032-0633(82)90003-4.

Yankovsky, V.A., Martyshenko, K.V., Manuilova, R.O., Feofilov, A.G., 2016. Oxygen dayglow emissions as proxies for atomic oxygen and ozone in the mesosphere and lower thermosphere. J. Mol. Spectrosc. 327, 209–231. https://doi.org/10.1016/j.jms.2016.03.006.

Yankovsky, V., Manuilova, R., 2018. Possibility of simultaneous $[O_3]$ and $[CO_2]$ altitude distribution retrievals from the daytime emissions of electronically-vibrationally excited molecular oxygen in the mesosphere. J. Atmos. Sol. Terr. Phys. 179, 23–33. https://doi.org/10.1016/j.jastp.2018.06.008.

Yankovsky, V., Vorobeva, E., Manuilova, R., 2019. New techniques for retrieving the [O(3P)], [O3] and [CO2] altitude profiles from dayglow oxygen emissions: Uncertainty analysis by the Monte Carlo method. Adv. Space Res. 64 (10), 1948–1967. https://doi.org/10.1016/j.asr.2019.07.020.

Yankovsky, V., 2020. The effect of atmospheric temperature on the calculations of the intensity of oxygen emissions in the framework of the Barth mechanism: sensitivity study. EGU General Assembly 2020, Online, 4–8 May 2020. https://doi.org/10.5194/egusphere-egu2020-57.